THE JOURNAL OF PHYSICAL CHEMISTRY C

Article

pubs.acs.org/JPCC

Tailoring Optical Properties of Silicon Nanowires by Au Nanostructure Decorations: Enhanced Raman Scattering and Photodetection

Renjie Chen,[†] Dehui Li,[†] Hailong Hu,[†] Yanyuan Zhao,[†] Ying Wang,[‡] Nancy Wong,[§] Shijie Wang,[§] Yi Zhang,[‡] Jun Hu,[‡] Zexiang Shen,[†] and Qihua Xiong*[,†,∥]

[†]Division of Physics and Applied Physics, School of Physical and Mathematical Sciences, Nanyang Technological University, Singapore 637371

[‡]Laboratory of Physical Biology, Shanghai Institute of Applied Physics, Chinese Academy of Sciences, Shanghai, 201800

[§]Institute of Materials Research and Engineering, Agency for Science, Technologies and Research, Singapore 117602

[∥]Division of Microelectronics, School of Electrical and Electronic Engineering, Nanyang Technological University, Singapore 639798

Supporting Information

ABSTRACT: Metallic nanoparticles (NPs) decorated semiconductor nanowires (NWs) heterostructures show significant promise in enhanced optical and opto-electrical properties due to the coupling of surface plasmon to nanowires. Here, we demonstrate a galvanic displacement based strategy to achieve *in situ* nucleation of Au nanoparticles and then postgrowth into higher order Au nanostructures such as dimers, nanorods, and nanoprisms along *the same* Si nanowires (SiNWs). The presence of Au nanostructures significantly enhances the optical properties of nanowires. Particularly, a 24 times enhancement of Si Raman scattering signal was achieved with a Au dimer decoration. A Au nanorod aligned in parallel along nanowire strongly enhances the anisotropy of Si Raman scattering, with more than 28 times stronger signal under parallel polarization than that under perpendicular polarization, demonstrating for the first time the surface plasmon enhanced antenna effect. In addition, we demonstrate that surface plasmon enhances photocurrent of SiNW by almost 100%, which is higher than previous reports. Our studies show that SiNWs decorated with metallic nanostructures by *in situ* galvanic displacement exhibit significant promise toward high efficiency photodetection and light harvesting applications.

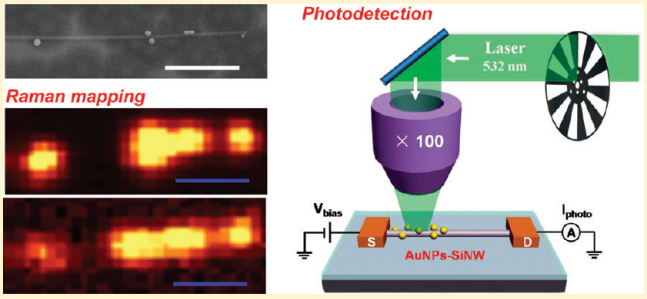

INTRODUCTION

Recently, increasing interests have been drawn on metallic nanoparticles decorated semiconductor nanomaterials, especially SiNWs, due to the expanded functionality and considerable promise in a wide range of applications. For instance, selectively deposited metallic nanoparticles can be used for a secondary growth of nanowires, which enables the unconventional synthesis of semiconductor heterostructures with encoded novel properties for logic gates and addressable transistors.[1−3] Metallic nanoparticles−SiNW heterostructures also exhibit enhanced interaction between photons and nanowires, leading to excellent photocatalytic properties. For example, Pt NPs-decorated SiNW arrays have been shown to enhance photoconversion efficiency in photoelectrochemical solar cells.[4] What makes these heterostructures more unique is the interaction between surface plasmon resonance of noble metal (e.g., Pt, Ag, or Au) and the SiNWs. These metal nanocrystals can not only serve as hot spots supported by the large area of the nanowire surface but also improve the optical and opto-electrical properties of the semiconductor nanowires themselves. Thus, extended research and applications have also been carried out on surface-enhanced Raman scattering (SERS)[5−8] and biosensing.[9] However, in this system, optimal interface with close interconnection is crucial for applications based on plasmon enhancement, since the localized electromagnetic field on the metal surface exponentially decreases with a characteristic decay length scale of ∼2 nm.[10]

Galvanic displacement is an effective way to decorate SiNWs with metallic nanoparticles, such as Au or Ag, with clean and heteroepitaxial interface.[11] In this process, silicon nanowire surface serves as both the template for particles decoration and the source of electrons that reduce the metal ions in solution. Fresh SiNW surface can provide the necessary reduction potential to facilitate the formation of uniform Ag or Au nanoparticles.[2,12] Upon the supply of hydrofluoric (HF) acid, continuous metallic ion reduction can be sustained and

Received: October 24, 2011
Revised: January 19, 2012
Published: January 24, 2012

postgrowth of metallic nanostructures is facilitated. By applying this method, we successfully achieved the heteroepitaxial growth of silver nanoparticles onto SiNWs with an average diameter of 25 nm in previous work and demonstrated a 7 times Si Raman signal enhancement by a single Ag nanoparticle.[12]

Though a few studies have been reported to explore controllable particle size and coverage density by tuning HF concentration and reaction time, the irregular morphology and random aggregation of the deposited NPs can result in inefficient SERS effect and a poor reproducibility of the Raman signal.[7] Thus, we aim at tailoring the metal nanoparticles on SiNWs into higher order geometries and investigating the influence of the nanostructure morphology on the plasmonic coupling efficiency.

In this paper, we demonstrate a galvanic displacement based strategy to achieve *in situ* nucleation of Au nanoparticles and then postgrowth into higher order nanostructures such as dimers, nanorods, and nanoprisms (Figure 1). Raman

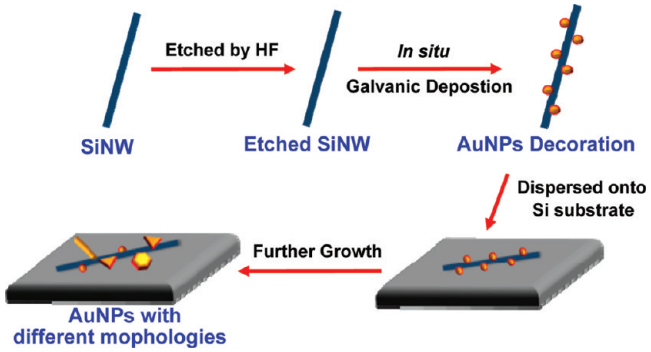

Figure 1. Schematic diagram for Au nanoparticle decorations on SiNWs with a two-step method, including the *in situ* galvanic displacement and a subsequent growth into different morphologies.

scattering and mapping were carried on an individual SiNW decorated with Au nanostructures. It shows that the Raman signal of a Si nanowire can be significantly enhanced by a factor of larger than 24 with a Au dimer decoration, while a gold nanorod aligned along nanowire in parallel strongly enhances the anisotropy of Si Raman scattering.

To bring the plasmon enhancement applications one step further, we also demonstrate the plasmon enhanced photodetection of SiNWs. The photocurrent increases by almost 2-fold with Au nanoparticle decorations, suggesting significant promises in visible light detection.

EXPERIMENTAL SECTION

Chemical Vapor Deposition (CVD) Growth of SiNWs. In this work, SiNWs were synthesized by the widely used vapor−liquid−solid mechanism in a low-pressure CVD system. Commercial 30 nm Au nanoparticles (Ted Pella) were dispersed onto silicon substrates as catalysts. 40 sccm silane and 50 sccm diborane (100 ppm in H_2) were used as Si source and doping gases, respectively. The growth was carried out at 440 °C for 10 min at a pressure of 70 Torr under 400 sccm H_2 carrier gas environment.

***In Situ* Galvanic Deposition of Au Nanoparticles onto SiNWs.** First, the SiNWs on growth substrate were dispersed into isopropanol by ultrasonicating. The amount of SiNWs for each reaction was fixed. Then SiNWs were etched in 1% HF aqueous solution to remove the surface SiO_2 layer, immediately followed by a 10−15 min centrifugation at 14 000 rpm in order to precipitate nanowires. After that, the newly etched SiNWs were added into a 1 mL $HAuCl_4$ solution with different concentrations (20, 50, and 80 μM). The reaction lasted for 10 min, followed by centrifugation and rinsing for a few times.

Postgrowth of Au Nanoparticles into Different Morphologies. The growth was carried on by dispersing the as-decorated Si NWs sample (i.e., those grown with $HAuCl_4$ concentration 20 μM) onto a silicon substrate with a native oxide layer, and then the substrate was immersed in the reaction solution containing 0.08 M hexadecyltrimethylammonium bromide (CTAB), 80 μM $HAuCl_4$, and 400 μM ascorbic acid. The reaction was conducted at room temperature, and the particle growth was controlled by elongating the reaction time from 20 min to 22 h.

Si Field Effect Transistor (FET) Device Fabrication. The SiNW FET devices were fabricated using electron-beam lithography (EBL) to define the source and drain electrodes, followed by metal evaporation and lift-off. Ni was used as the contact metal, followed by a rapid thermal annealing process in order to form an ohmic contact. After a second EBL step, selective *in situ* AuNPs deposition was carried out within the opened window of e-beam resist, which exposes part of the nanowire to the reaction solution. A similar galvanic decoration process was used as mentioned before, while HF etching time was minimized to 10−15 s.

Sample Characterizations. Scanning electron microscopy (SEM) was conducted using a JEOL 7001F microscope. Transmission electron microscopy (TEM) imaging and elemental mapping were carried out under a JEOL 2100 microscope. Raman mapping were taken using a WITEC CRM200 confocal Raman microscopy system. The excitation laser was a double-frequency Nd:YAG laser (532 nm, CNI Laser) with a laser power below 1.0 mW. Photocurrent measurements were carried out on a homemade setup as schematically shown in Figure 6a. The incident 532 nm laser was modulated by an optical chopper with a frequency of 37 Hz, and the source-drain bias was provided by a DAQ card. Photocurrent was amplified by a preamplifier (DL Instruments, 1211) and then recorded by a lock-in amplifier. Hence, any DC current will be filtered, and the resulting photocurrent is only due to photogenerated carriers. The laser spot was smaller than 2 μm and can be accurately focused onto certain part of the device by a 100× objective.

RESULTS AND DISCUSSION

The simple procedure we developed for decorating gold nanoparticles with a variety of morphologies on SiNWs is shown schematically in Figure 1. In the first step, the galvanic displacement method is used to decorate silicon nanowires with small gold nanoparticles, in which gold ions are reduced with electrons supplied by reaction on the newly etched SiNWs surface (i.e., half-cell reaction: $Si + 6F^- \rightarrow SiF_6^{2-} + 4e^-$). The particle size and coverage density can be tuned by applying different initial $HAuCl_4$ concentrations (i.e., 20, 50, and 80 μM). The results show that, with a higher concentration of gold ions, the particle size is increased while the density is slightly decreased.

We then carried on a second step to continue the particle growth, by elongating the reaction time with the presence of CTAB. In this process, the *in situ* decorated nanoparticles (Figure 2a) act as small seeds to initiate the secondary growth,

dx.doi.org/10.1021/jp210198u | J. Phys. Chem. C 2012, 116, 4416−4422

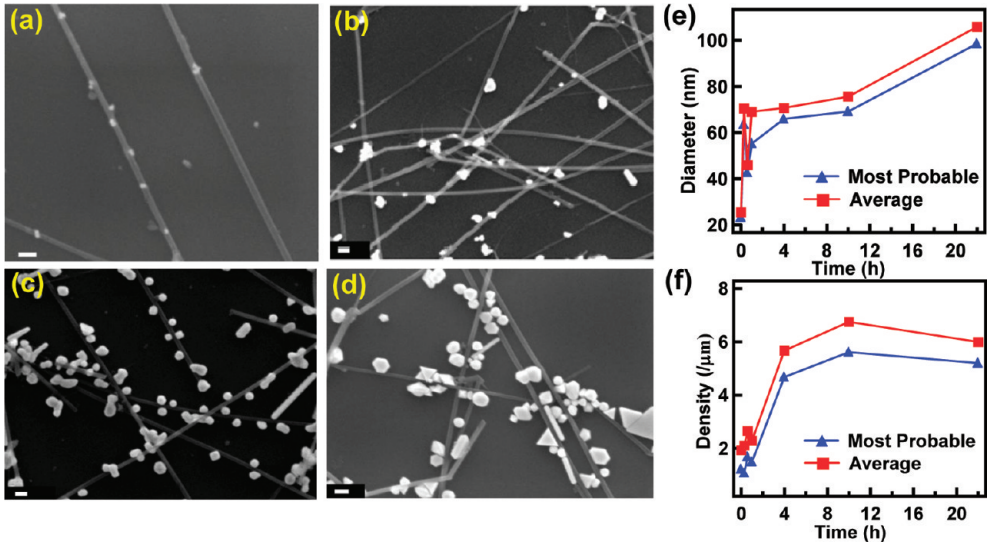

Figure 2. SEM images and statistic results for the evolution of morphology, size, and density of Au nanostructures on SiNWs. (a) Au nanoparticles on SiNWs by *in situ* galvanic displacement. (b–d) After different particle-growth stage, with reaction duration of 1, 4, and 22 h, respectively. Scale bars are all 100 nm. (e, f) Statistics of diameter and density of nanoparticles versus time.

and the CTAB serves as good cationic surfactant for steric stabilization and shape control. We found that this process can effectively increase the nanoparticle size. In addition, higher order nanostructures such as nanorods, prisms, or dimers can be formed on nanowires.

SEM images are shown in Figure 2b–d for 1, 4, and 22 h growth, respectively, and Figure 2e,f displays the statistical results of size distribution and particle density variation trend as a function of reaction time. At the initial 1 h, there is no significant shape change of gold nanoparticles, while the size of particles increases very rapidly. After 4 h reaction, some regular-shaped particles start to form with an increased coverage density. At longer reaction time, e.g., 22 h, different shaped (i.e., triangular or hexagonal prisms, nanorods, dimers, etc.) particles could easily be found, and particle density remains nearly constant.

In order to carry out TEM characterizations on those Au-nanocrystal SiNW heterostructures, we performed similar growth directly on Si_3N_4 membrane TEM grids with a reaction time of 10 h. Figure 3a shows a typical TEM image of SiNWs decorated with Au nanostructures. To confirm the composition of these nanoparticles on SiNWs, elemental mapping was carried out. Figure 3b displays the Au M edge mapping image taken under scanning transmission electron microscopy (STEM) mode, and the inset is the corresponding bright field TEM image of the same area. Clear contrast between Si and Au can be identified, suggesting a pure Au nanoparticle phase decoration. The interface between a gold nanorod and the SiNW in Figure 3c indicates a gap of less than 1 nm, which is induced by the surface oxidation of SiNW during reaction. This close interconnection ensures the localized surface plasmon resonance of gold particles efficiently couples into the SiNW.

Raman scattering and mapping were carried out on individual SiNWs with high order Au nanostructures decoration, in order to understand how the scattering properties depend on morphology of Au nanostructures. As shown in Figure 4a, this SiNW is more than 3 μm long, decorated with four different types of Au nanostructures: a

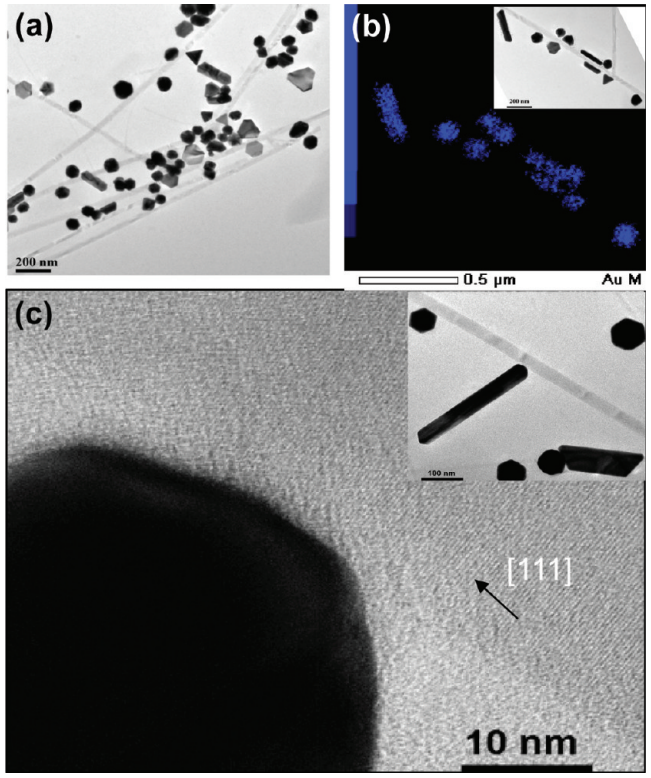

Figure 3. Au nanostructure decorated SiNWs on Si_3N_4 substrate. (a) Typical TEM image of Au nanostructures with a variety of shapes that are decorated on SiNWs. (b) Au M edge elemental mapping, confirming the nanoparticles are indeed Au (inset, the corresponding TEM image of the same position). (c) HRTEM image showing the interface between Au nanorod and Si nanowire. The inset is the low magnification TEM of this Au nanorod–SiNW heterostructure.

spherical nanoparticle, a nanoparticle dimer, a cylindrical nanorod, and a triangular prism.

When integrated from 600 to 3800 cm^{-1} (where the Raman signal from the substrate GaAs and the Si nanowire can both be excluded) (Figure 4b), the mapping signal reveals the strong

dx.doi.org/10.1021/jp210198u | J. Phys. Chem. C 2012, 116, 4416–4422

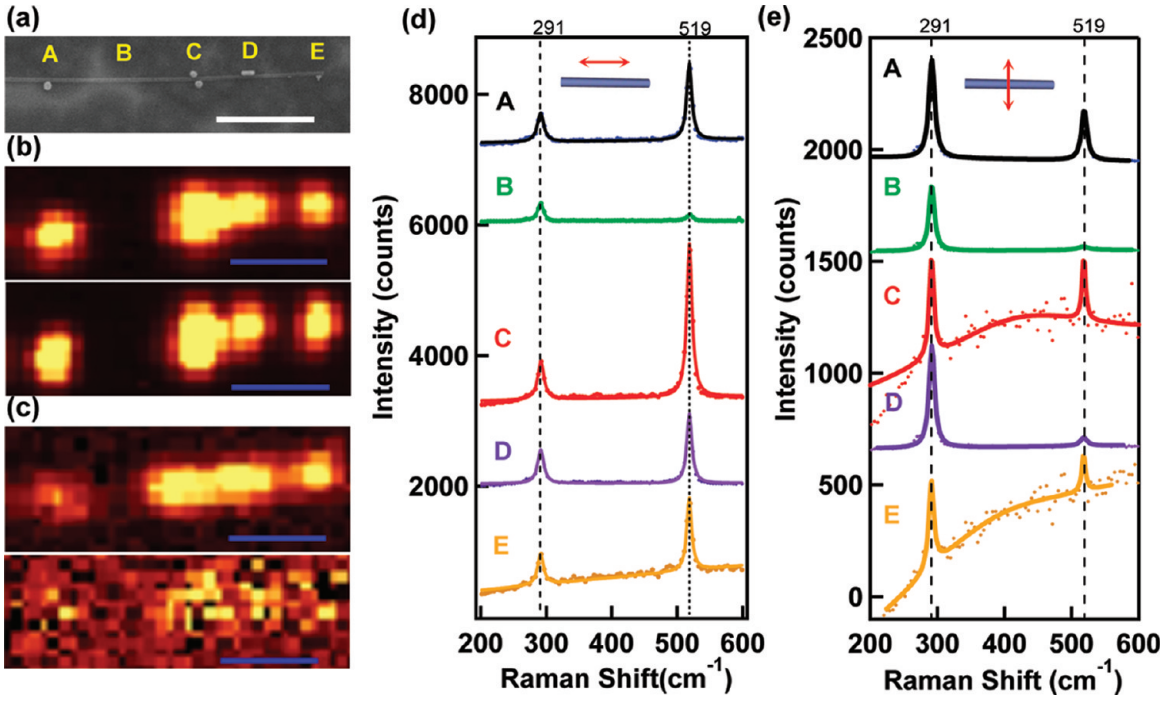

Figure 4. Raman mapping of an individual SiNW decorated with a series of Au nanostructures. (a) SEM image of a SiNW, decorated with Au nanostructures of various morphologies. Spot B indicates the bare SiNW, while A, C, D, and E spots represent a gold spherical nanoparticle, a nanoparticle dimer, a cylindrical rod, and a triangular prism, respectively. (b) Raman mapping of nanowire shown in (a) integrated from 600 to 3800 cm^{-1} for parallel (up) and perpendicular (down) polarizations, corresponding to Au scattering. (c) Raman mapping of the same nanowire integrated from 490 to 550 cm^{-1} for parallel (up) and perpendicular (down) polarizations, corresponding to the Si first-order TO Raman band. All the scale bars are 1 μm. (d, e) Raman spectra collected from spots A–E, with (d) parallel and (e) perpendicular polarizations, and the curves are offset accordingly for clarity.

scattering from gold nanoparticles, which can be used to identify the location of each particle. The polarization does not show much influence on the gold scattering intensity with only a slight profile change, however, the strong polarization dependence of Si signal is exhibited in Figure 4c when the mapping signal is integrated from 490 to 550 cm^{-1}. When the laser is polarized along the nanowire, the Si signal is in a high contrast with the background and the enhancement from each particle is pronounced. However, when the laser polarization is perpendicular to the nanowire, the Raman scattering is completely suppressed along the nanowire, which is consistent with the well-known antenna effect.[13,14]

Three factors contribute to the optical properties of gold nanoparticles: size, shape, and dielectric environment.[15−17] When those nanoparticles are hybridized with semiconductor materials, the interface is another issue that should be considered, as the distance may degrade the plasmon coupling into semiconductor materials dramatically.[7] Here in our situation, all the gold nanocrystals are present in the same dielectric environment with a close and clean interface to SiNWs by galvanic displacement reaction. In addition, for small NPs (<100 nm), size will not notably influence the optical response of NPs and the plasmon resonances depend primarily on the NP's shape.[15] For these reasons we mainly focus on the influence of gold nanoparticle geometry on the Raman enhancement of SiNWs.

To study the enhancement factor arising from Au nanostructures with different morphologies, the spectra collected from each spot with two polarization orientations were displayed in Figure 4d,e with multiple-Lorentzian peak fitting presented. The 291 cm^{-1} peak originates from the longitudinal optical (LO) phonon modes of GaAs substrate,[18] and the 519 cm^{-1} is a 3-fold degenerated transverse optical (TO) phonon modes of Si. For some nanowires, *in situ* galvanic displacement can also introduce another strong Raman band located around 495 cm^{-1} due to polycrystalline defect formation, which has been discussed in detail previously in Ag-decorated SiNWs.[12] The Raman spectra clearly show considerable enhancement from each of the Au-decorated spots (A, C, D, and E) compared to the bare Si signal (spot B). The different intensities of Si TO peak demonstrate the diverse enhancement capabilities from Au particles with different morphologies. By analyzing the multiple-Lorentzian peak fitting data, we listed the enhancement ratio of each particle decorated portion against the bare Si spot (see Table S1).

For the single spherical particle ~80 nm at spot A, a Si TO peak enhancement of 12.1 times was observed when light was polarized along the Si nanowire, which is higher than previous report with Ag nanoparticles.[12] This is probably due to stronger coupling between the incident laser (532 nm) and Au surface plasmon, as silver spherical particles normally have a higher surface plasmon resonance frequency.

When two nanoparticles with size of ~70 nm are aggregated on both sides of the SiNW to form a dimer structure, as shown at spot C, the Raman signal was dramatically enhanced by a factor of 24.3. Considerable studies have been done on the coupling between metal nanostructures, as the strong field confinement can be achieved in these nanoscale gaps.[19−22] Some well-designed dimer structures are also carried out for SERS applications.[23,24] So, these nanoparticle dimer structures synthesized in a wet chemistry offer another bottom-up

dx.doi.org/10.1021/jp210198u | J. Phys. Chem. C 2012, 116, 4416−4422

approach to effectively couple to semiconductor nanomaterials and therefore enhance the optical properties significantly.

Another interesting question is how the optical properties of nanowires are affected if the nanoparticle is replaced by lower symmetry nanostructures, such as prisms or nanorods. When spherical nanoparticles are evolved into nanorods, the plasmon resonance splits into the longitudinal mode and the transverse mode, corresponding to long axis and short axis resonance, respectively,[16,25] and electromagnetic fields can be enhanced at the tips compared to spheres.[17,25,26] Moreover, when the nanorod has the long axis approaching the excitation wavelength, the optical phase can vary across the structure and retardation effects need to be considered.[27] Here, the cylindrical nanorod (~145 nm long with a diameter of ~47 nm) at spot D yielded an enhancement factor of 11 which does not show much difference compared to the single spherical particle. Surprisingly, however, the Si TO peak intensity is more than 28 times stronger in parallel polarization at this spot than that in perpendicular polarization, which means that the nanorod structure parallel adhesive to the SiNW dramatically enhanced the anisotropy of Si Raman signal (Figure 5). Since

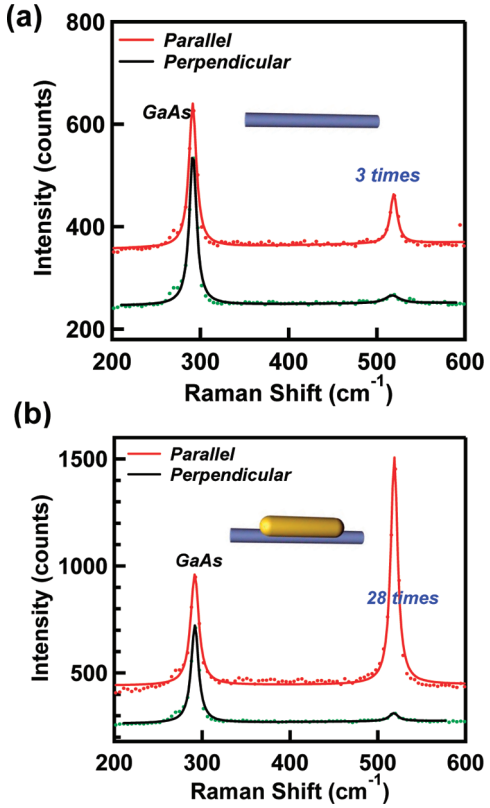

Figure 5. Polarization-dependent Raman scattering spectra from (a) bare SiNW at spot B and (b) Au nanorod decorated SiNW at spot D, respectively. The 291 cm^{-1} Raman peak is from LO phonon modes due to GaAs substrate. The curves for parallel polarization in both (a) and (b) are offset vertically for clarity.

the laser we used cannot efficiently excite the longitudinal mode, we tentatively attribute this strong enhancement to the large surface area of nanorod−nanowire interconnection and the coupling between incident laser and surface plasmon polariton (SPP) along the nanorod long axis. Previously, the SPP-enhanced SERS effect was observed in Au−ZnO core−shell nanorod structures,[28] and plasmon-enhanced fluorescence was found to be strongly dependent on polarization with gold nanorod structures.[29] So here, for the first time we observed that the antenna effect of SiNWs was significantly enhanced due to anisotropic plasmon coupling. For the case of triangular gold prisms, surface plasmon resonance is mainly determined by in-plane dipole excitation associated with the sharp tips.[30] Here, the triangular particle with a side length of ~54 nm gave an enhancement factor of 12.

From the comparison we can conclude that the dimer particles are the most effective structure for enhancing Raman scattering along both polarization directions, while nanorod−nanowire hybrid structures significantly enhance the antenna effect, where the Raman scattering is further anisotropic when the nanorod is aligned parallel to nanowires. These phenomena are interesting not only for Raman enhancement study but also for other applications, such as plasmon-enhanced absorption, luminescence, etc.

Recently, semiconductor nanowires have been demonstrated to harvest solar energy efficiently toward applications in photovoltaics or photocatalysis, especially the vertically aligned arrays with periodic arrangement.[31,32] In addition, Si nanowires have also been reported as a polarization-sensitive, high-resolution photodetector in the visible range.[33] By introducing metallic nanoparticles, the functionality of nanowires can be further extended, such as enhanced absorption and emission as recently demonstrated in the literature.[34] To further evaluate how Au nanostructure decoration affects the optical and opto-electrical properties, we investigate the photocurrent response of the single SiNW FET with and without nanostructure decorations. This was achieved by decorating Au nanoparticles on part of a SiNW FET, while the remaining part of the wire was masked by PMMA resist.

In order to selectively illuminate the segment of SiNW with and without Au nanostructure decorations (schematically shown in Figure 6a), a 100× objective was employed to accurately locate the laser spot. The device channel was designed ~4 μm long to minimized the possible photoresponse from the electrode contacts because extra charge separation will be induced by the band edge bending near the electrode.[33] The actual device is shown in Figure 6b with partial Au nanoparticle decoration (i.e., region M, compared with bare Si part, region N).

As shown in Figure 6c, the dark current increases linearly with source-drain voltage, indicating a good ohmic contact. The slopes of AC photocurrent versus bias voltage are significantly different with and without Au nanoparticles decoration (Figure 6d). When the laser is illuminated at region M with nanoparticle decoration, the slope (i.e., photoconductance) is 230 nS, which is much higher than that at region N (129 nS). This illustrates that Au nanoparticles can significantly improve the photosensitivity of SiNW device. In order to clearly see this trend, the switching characteristics were investigated with light illuminating at region M and N, respectively (Figure 6e). It is observed that the photocurrent increases almost 2 times with gold nanoparticles decoration, resulting from strongly enhanced local field induced by surface plasmon resonance. A previous report showed a 20% increase of photocurrent by single particles dispersed from commercial colloid gold nanoparticles solution onto SiNWs.[35] Their simulation shows an exponential decay of absorption enhancement as the separation between particle and nanowire is larger than 2 nm. Our results indicate that a higher plasmon enhance efficiency can be achieved with nanoparticles decorated by galvanic displacement because this

dx.doi.org/10.1021/jp210198u | J. Phys. Chem. C 2012, 116, 4416−4422

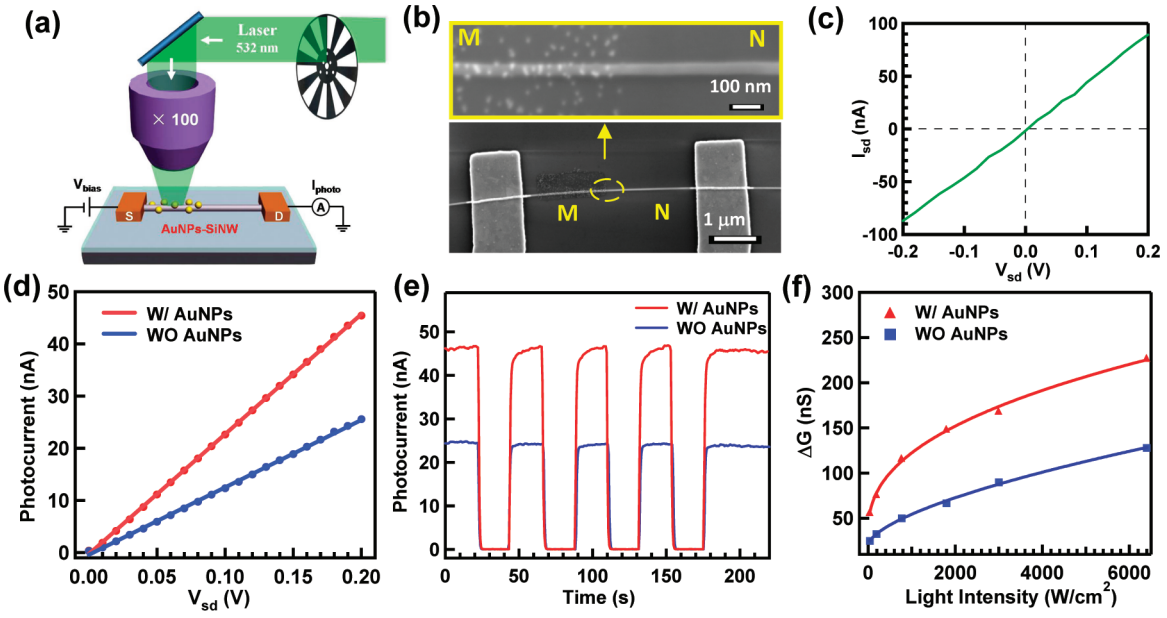

Figure 6. Photoconductance improvement of SiNW FET by Au nanoparticles decoration. (a) Schematic for photocurrent measurement of single SiNW FET device, the SiNW is partially decorated with gold nanoparticles and the 532 nm laser spot was around 1 μm. (b) SEM images of a SiNW FET device with partial Au-NP decoration (bottom) and the zoom in image (up). (c) DC $I-V$ curve of the device, showing the linear behavior of dark current versus bias voltage. (d) Photocurrent of the corresponding device, measured with a light intensity of 6400 W/cm^2. (e) Time-dependent photocurrent response to 532 nm laser, measured with light intensity of 6400 W/cm^2 and 0.2 V bias voltage. (f) Photoconductance response to the light intensity, measured with a 0.2 V bias voltage. All the current or conductance data shown in (d–f) are taken from ac measurements by a lock-in amplifier.

method offers an optimized interface between AuNPs and SiNW with minimized interconnection. Though some nonspecific gold particles are also observed beside the SiNW, they are too far away to contribute to the plasmon enhancement, and their scattering effects are negligible due to the small size.[36]

The dependence of photocurrent on the light intensity was also studied, which was illustrated in Figure 6f. The photocurrent I vs laser power P curves can be well fitted by a simply power law:

$$I = AP^{\chi}$$

where A is a constant for certain wavelength and χ determines the response of photocurrent to the light intensity.[37] In our measurements, χ is 0.41 and 0.62 for region M and region N, respectively. For both regions, the value of χ is less than one. This nonunity value was previously also observed in ZnO nanowire[38] and CdS nanobelt[37] devices. A number of processes involved can give rise to this nonunity, including photocarrier generation, trapping, recombination, and carrier transport within semiconductors.[39] The smaller value of χ in region M compared to region N is not clear yet. Possible reasons include photocurrent saturation caused by the high doping concentration or surface states introduced by the contact of Au nanoparticles with Si nanowire.

Overall, SiNW with AuNPs decoration shows higher efficiency for plasmon-enhanced photocurrent, which not only provides a way to improve photodetection of semiconductor nanowires but also shows promises in light harvesting.

CONCLUSION

In conclusion, Au nanostructures with a variety of morphologies can be successfully decorated onto SiNWs by a two-step method. Galvanic displacement is employed to first form nanoparticle seeds at the metal–semiconductor interface. In a second reduction step, the nanostructure size, shape, and coverage density can be tailored. Raman scattering and mapping are carried out on individual SiNW decorated with Au nanoparticles of different geometries. A 24 times enhancement of Si Raman signal is exhibited with a Au dimer structure due to the strong electromagnetic field confinement. We also find that the gold nanorod aligned parallel to nanowire strongly enhanced the anisotropy of Si Raman scattering with more than 28 times stronger signal under parallel polarization, which is the first demonstration of surface plasmon enhanced antenna effect. At last, we demonstrate that the photocurrent of SiNW is enhanced by almost 100% by the plasmonic near-field response of gold nanoparticles. Our studies show that SiNWs decorated with metallic nanostructures by *in situ* galvanic displacement exhibit significant promise toward high efficiency photodetection and light-harvesting applications.

ASSOCIATED CONTENT

Supporting Information

Additional SEM images and statistical results. This material is available free of charge via the Internet at http://pubs.acs.org.

AUTHOR INFORMATION

Corresponding Author

*E-mail: Qihua@ntu.edu.sg.

Notes

The authors declare no competing financial interest.

ACKNOWLEDGMENTS

Q.X. thanks the strong support from Singapore National Research Foundation through Singapore 2009 NRF fellowship grant (NRF-RF2009-06), a start-up grant support

(M58110061), and the New Initiative Fund (M58110100) from Nanyang Technological University. Y.Z. thanks the support from National Science Foundation of China (No. 90923002).

REFERENCES

(1) Wang, D.; Qian, F.; Yang, C.; Zhong, Z.; Lieber, C. M. *Nano Lett.* **2004**, *4*, 871.
(2) Jiang, X.; Tian, B.; Xiang, J.; Qian, F.; Zheng, G.; Wang, H.; Mai, L.; Lieber, C. M. *Proc. Natl. Acad. Sci. U. S. A.* **2011**, *108*, 12212–12216.
(3) San Paulo, Á.; Arellano, N.; Plaza, J. A.; He, R.; Carraro, C.; Maboudian, R.; Howe, R. T.; Bokor, J.; Yang, P. *Nano Lett.* **2007**, *7*, 1100.
(4) Peng, K.; Wang, X.; Wu, X.; Lee, S. *Nano Lett.* **2009**, *9*, 332.
(5) Leng, W.; Yasseri, A. A.; Sharma, S.; Li, Z.; Woo, H. Y.; Vak, D.; Bazan, G. C.; Kelley, A. M. *Anal. Chem.* **2006**, *78*, 6279.
(6) Zhang, B.; Wang, H.; Lu, L.; Ai, K.; Zhang, G.; Cheng, X. *Adv. Funct. Mater.* **2008**, *18*, 2348.
(7) Fang, C.; Agarwal, A.; Widjaja, E.; Garland, M. V.; Wong, S. M.; Linn, L.; Khalid, N. M.; Salim, S. M.; Balasubramanian, N. *Chem. Mater.* **2009**, *21*, 3542.
(8) Becker, M.; Stelzner, T.; Steinbrück, A.; Berger, A.; Liu, J.; Lerose, D.; Gösele, U.; Christiansen, S. *ChemPhysChem* **2009**, *10*, 1219.
(9) Kang, T.; Yoo, S. M.; Yoon, I.; Lee, S. Y.; Kim, B. *Nano Lett.* **2010**, *10*, 1189.
(10) Haynes, C. L.; McFarland, A. D.; Duyne, R. P. V. *Anal. Chem.* **2005**, *77*, 338A.
(11) Sayed, S.; Wang, F.; Malac, M.; Meldrum, A.; Egerton, R.; Buriak, J. *ACS Nano* **2009**, *3*, 2809.
(12) Peng, Z.; Hu, H.; Utama, M. I. B.; Wong, L. M.; Ghosh, K.; Chen, R.; Wang, S.; Shen, Z.; Xiong, Q. *Nano Lett.* **2010**, *10*, 3940.
(13) Xiong, Q.; Chen, G.; Gutierrez, H. R.; Eklund, P. C. *Appl. Phys. A: Mater. Sci. Process.* **2006**, *85*, 299.
(14) Chen, G.; Wu, J.; Lu, Q.; Gutierrez, H. R.; Xiong, Q.; Pellen, M. E.; Petko, J. S.; Werner, D. H.; Eklund, P. C. *Nano Lett.* **2008**, *8*, 1341.
(15) Noguez, C. *J. Phys. Chem. C* **2007**, *111*, 3806.
(16) Kelly, K. L.; Coronado, E.; Zhao, L. L.; Schatz, G. C. *J. Phys. Chem. B* **2003**, *107*, 668.
(17) Murphy, C. J.; Sau, T. K.; Gole, A. M.; Orendorff, C. J.; Gao, J.; Gou, L.; Hunyadi, S. E.; Li, T. *J. Phys. Chem. B* **2005**, *109*, 13857.
(18) Mahan, G. D.; Gupta, R.; Xiong, Q.; Adu, C. K.; Eklund, P. C. *Phys. Rev. B* **2003**, *68*, 073402.
(19) Romero, I.; Aizpurua, J.; Bryant, G. W.; García De Abajo, F. J. *Opt. Express* **2006**, *14*, 9988.
(20) Aćimović, S. S.; Kreuzer, M. P.; González, M. U.; Quidant, R. *ACS Nano* **2009**, *3*, 1231.
(21) Taychatanapat, T.; Bolotin, K. I.; Kuemmeth, F.; Ralph, D. C. *Nano Lett.* **2007**, *7*, 652.
(22) Ghenuche, P.; Cherukulappurath, S.; Taminiau, T. H.; van Hulst, N. F.; Quidant, R. *Phys. Rev. Lett.* **2008**, *101*, 116805.
(23) Nagasawa, F.; Takase, M.; Nabika, H.; Murakoshi, K. *Chem. Commun.* **2011**, *47*, 4514.
(24) Lee, S. Y.; Hung, L.; Lang, G. S.; Cornett, J. E.; Mayergoyz, I. D.; Rabin, O. *ACS Nano* **2010**, *4*, 5763.
(25) Sosa, I. O.; Noguez, C.; Barrera, R. G. *J. Phys. Chem. B* **2003**, *107*, 6269.
(26) Imura, K.; Nagahara, T.; Okamoto, H. *J. Am. Chem. Soc.* **2004**, *126*, 12730.
(27) Schuller, J. A.; Barnard, E. S.; Cai, W.; Jun, Y. C.; White, J. S.; Brongersma, M. L. *Nature Mater.* **2010**, *9*, 193.
(28) Sakano, T.; Tanaka, Y.; Nishimura, R.; Nedyalkov, N. N.; Atanasov, P. A.; Saiki, T.; Obara, M. *J. Phys. D: Appl. Phys.* **2008**, *41*, 235304.
(29) Ming, T.; Zhao, L.; Yang, Z.; Chen, H.; Sun, L.; Wang, J.; Yan, C. *Nano Lett.* **2009**, *9*, 3896.
(30) Hao, E.; Bailey, R. C.; Schatz, G. C.; Hupp, J. T.; Li, S. *Nano Lett.* **2004**, *4*, 327.
(31) Boettcher, S. W.; Spurgeon, J. M.; Putnam, M. C.; Warren, E. L.; Turner-Evans, D. B.; Kelzenberg, M. D.; Maiolo, J. R.; Atwater, H. A.; Lewis, N. S. *Science* **2010**, *327*, 185.
(32) Kelzenberg, M. D.; Boettcher, S. W.; Petykiewicz, J. A.; Turner-Evans, D. B.; Putnam, M. C.; Warren, E. L.; Spurgeon, J. M.; Briggs, R. M.; Lewis, N. S.; Atwater, H. A. *Nature Mater.* **2010**, *9*, 239.
(33) Ahn, Y.; Dunning, J.; Park, J. *Nano Lett.* **2005**, *5*, 1367.
(34) Achermann, M. *J. Phys. Chem. Lett.* **2010**, *1*, 2837.
(35) Hyun, J. K.; Lauhon, L. J. *Nano Lett.* **2011**, *11*, 2731.
(36) Cecilia, N. *Opt. Mater.* **2005**, *27*, 1204.
(37) Jie, J. S.; Zhang, W. J.; Jiang, Y.; Meng, X. M.; Li, Y. Q.; Lee, S. T. *Nano Lett.* **2006**, *6*, 1887.
(38) Kind, H.; Yan, H.; Messer, B.; Law, M.; Yang, P. *Adv. Mater.* **2002**, *14*, 158.
(39) Rose, A. *Concepts in Photoconductivity and Allied Problems*; Krieger: New York, 1978.